Plasma Shifts of Hydrogenic-Ion Lines

T. L. Pittman, P. Voigt, and D. E. Kelleher
National Bureau of Standards, Washington, D. C. 20234
(Received 13 November 1979)

Systematic red shifts for the Paschen α, β, and γ lines ($n = 4, 5, 6 \rightarrow n = 3$) of He II are observed over an electron density range of $(1-8)\times 10^{22}$ m^{-3}. The measurements are compared with combined estimates for plasma polarization and ion quadrupole effects. It is demonstrated that previous theoretical estimates have left out an important contribution to the polarization shift, which we estimate using the Debye model.

PACS numbers: 52.25.Ps, 32.70.Jz, 34.10.Hx, 52.20.Hv

The center of gravity of hydrogenic lines is unshifted by uniform electric fields. Inclusion of time-dependent effects in the electron and ion broadening of hydrogenic ions in plasmas has yielded negligible shifts.[1-3] Thus early results[4] suggesting shifted hydrogenic lines generated considerable interest. These so-called "plasma polarization" shifts (PPS) have been the subject of several recent reviews,[5-7] and we refer the reader to them for a detailed discussion.

In this Letter we report red shifts for the Paschen α, β, and γ lines of HeII over an electron density range of $(1-8)\times 10^{22}$ m^{-3}. We believe these to be the first observations of systematic red shifts of hydrogenic ion lines. After a description of the experiment, we shall compare the measured results with theoretical shifts that include both ion quadrupole effects and an estimate of the effect of emitting-ion–plasma correlations. With one exception,[8] the effect of plasma polarization by the emitting ion is not considered in current Stark-broadening theories.

The plasma source is a pulsed arc (Z discharge) consisting of a cylindrical quartz tube of 22 mm i.d. with vacuum-fitted end electrodes separated by 90 mm. The electrodes include a 6-mm central bore for end-on observations through quartz windows. The discharge current is supplied by an undamped, lumped delay-line system of eight 15-μF capacitors and inductors. The current waveform approximates a square wave with a 10 μsec rise time, 130 μsec half-period, and a 0.5 msec decay rate. The current is approximately 5–6 kA during the first half-cycle for a 5 kV charging voltage. Emission of HeII lines is observed during this period.

The line spectrum was recorded on the 500 calibrated channels, each 25 μm wide, of the image-intensified optical multichannel analyzer (OMA). The OMA detector head was mounted at the exit plane of a $\frac{3}{4}$-m spectrometer having a 3600-line/mm holographic grating resulting in a reciprocal linear dispersion of 0.0025 nm per channel at 468.6 nm. A 1.1-kV gate pulse to the OMA detector time integrated the line emission over a 10-μsec interval at 50 μsec into the first half-cycle of discharge current. The OMA was interfaced to a laboratory minicomputer for detailed data processing and reduction.

The dispersion and absolute wavelength were calibrated against a known spectral source (usually a thorium or iron lamp) accurate to within a single channel bandwidth. The relative sensitivity of the diode array was obtained with a calibrated tungsten lamp for 468.6 nm and a deuterium lamp for the lower wavelengths. The calibrations were recorded with the OMA operating in the continuous mode. Different OMA operating characteristics due to electrostatic focusing variations between the gated and continuous mode can occur if the high-voltage signals to the OMA detector head are not the same. These differences were measured by observing in each mode a thorium-lamp spectrum consisting of at least ten narrow lines spaced across the detector diode array. The spectrum observed in the gated mode expanded about the diode array center when compared with the time-independent mode. Fitting the measurements to a quadratic function allowed for the correction of the calibrations on a channel-by-channel basis. The effect of the corrections was to slightly alter (< 3% at half width at half maximum) the width of a broad line centered on the diode array. The instrumental profile of the system (spectrometer and OMA) is measured using He I lines from a Geissler tube. Instrumental (treated as Gaussian) and Doppler widths combine giving a total Gaussian width of about 0.02 nm. The "Voigt" deconvolution of this Gaussian from the experimental profiles (assumed Lorentzian in this procedure) resulted in at most an 8% correction to the measured half-widths. Temperatures of 45 000 and 41 500 K were measured end on and side on, respectively, from the ratio of the He I

318.7-nm and the He II 320.3-nm total line intensities under the assumption of local thermodynamic equilibrium. The lower side-on temperature may be partly due to increased He I emission from cooler boundary layers. As the helium-gas filling pressure was varied (2 to 10 Torr), the capacitor charging voltage was adjusted to maintain a constant (< 10%) temperature over the electron density range.

A He-Ne laser quadrature interferometer[9] measured the electron density end on along the central chord of the plasma. Spatially resolved end-on measurements (with use of the interferometer) and side-on observations (of He II line half-widths) indicate a uniform plasma (< 10% variations) both radially over a 6 mm diameter and longitudinally between the electrodes. Probe measurements indicate an exponentially decaying plasma within the electrode bores. The decay length is approximately 2 cm giving an effective plasma length of 12.8 ± 0.6 cm.

We estimate the time-average effects of plasma polarization by the emitting ion with a simple Debye shielding model. The Debye potential at a distance r from a one-electron ion of nuclear charge Z is

$$\varphi^{D}(r) = e(Z-1)r^{-1}\exp(-r/D), \tag{1}$$

where the Debye radius

$$D = [kT/4\pi e^2(N_e + \textstyle\sum_i N_i Z_i'^2)]^{1/2}. \tag{2}$$

N_e is the electron density; Z_i' is the net charge of the plasma ion. General validity criteria for the Debye model are discussed by Griem.[10]

After subtracting the potential due to the nucleus and bound electron, we arrive at the perturbation potential for the bound electron:

$$\varphi_p^{D}(r) = e(Z-1)r^{-1}[\exp(-r/D) - 1] \tag{3}$$

$$= [-e(Z-1)/D] + [e(Z-1)/2D^2]r - \ldots . \tag{4}$$

Since $\varphi_p^{D}(r)$ is spherically symmetric, the perturbation matrix is diagonal in the spherical representation of the hydrogenic wavefunctions. In this case the first-order perturbation energy shift is simply

$$\Delta E_{nl} = \langle nl|[-e\varphi_p(r)]|nl\rangle . \tag{5}$$

Substituting the hydrogenic value[11] for $\langle r\rangle$ gives

$$\Delta E_{nl} = e^2\frac{(Z-1)}{D} - \frac{e^2(Z-1)a_0}{4D^2Z}[3n^2 - l(l+1)] + \ldots . \tag{6}$$

Shifts for nonhydrogenic species, with ionization potential E_{IP}, can be estimated with use of $n^* = [Z^2E_H/(E_{IP} - E_{nl})]^{1/2}$ in the above equation. For hydrogenic ions we can perform a weighted average (with respect to magnetic quantum number) over l: $\langle l(l+1)\rangle = \frac{1}{2}(n^2-1)$ (for low N_e or high Z, fine-structure splitting must be accounted for). From Eq. (6) the plasma polarization shift in wavelength, $\Delta\lambda^{D}$, for a transition $n \to n'$ of wavelength λ in a hydrogenic ion of nuclear charge Z can be expressed to first order in $\langle r\rangle/D$ as

$$\frac{\Delta\lambda^{D}}{\lambda} = \frac{5}{4}\frac{Z-1}{Z}\left(\frac{a_0nn'}{ZD}\right)^2 . \tag{7}$$

Comparison with previous PPS models, which generally predicted blue shifts, is facilitated by expressing the perturbation potential in terms of the polarized charge density, $\rho_p(r)$. The Green's-function solution to the spherically symmetric Poisson equation is

$$\varphi_p(r) = \frac{4\pi}{r}\int_0^r \rho_p(r')r'^2dr' + 4\pi\int_r^\infty \rho_p(r')r'dr' . \tag{8}$$

For example, substitution of $\varphi_p^{D}(r)$ into the Poisson equation yields the Debye polarization charge density, $\rho_p^{D}(r) = -\varphi^{D}(r)/4\pi D^2$. Conversely, inserting $\rho_p^{D}(r)$ into (8) returns $\varphi_p^{D}(r)$. Previous theoretical estimates of PPS have started with various models for $\rho_p(r)$ (see the reviews cited above), and computed shifts from the expression $\Delta E_n = 2E_H Z\Delta Z/n^2$, where $\Delta Z = (4\pi/e)\int_0^{\langle r\rangle}\rho_p(r)r^2dr$ is the shielding charge inside the Bohr orbital. In the approximation that $\langle\varphi_p(r)\rangle = \varphi_p(\langle r\rangle)$, this expression for ΔE_n is equivalent to the first term in (8). The second term, i.e., the interaction of the bound electron with the polarized plasma *outside* the Bohr orbital, has been left out. The importance of this latter contribution can be seen by writing (8) as

$$\varphi_p(r) = (4\pi/r)\int_0^r \rho_p(r')(r'^2 - rr')dr' + \text{const.} \tag{9}$$

Here we have used the fact that the asymptotic r dependence of any physical $\rho_p(r)$ is such that $\int_0^\infty \rho_p(r)r\,dr$ is a finite constant [equal to $-e(Z-1)/D$ in the Debye model] and as such does not contribute to a shift in transition energies. For $\rho_p(r) \sim \sum_k a_k r^k$ near the origin, the integral in (9) is defined only for $k_{min} > -2$. For each such k val-

ue, the integral of the second term in (9) is a factor $(k+3)/(k+2)$ larger than that of the first term. Thus, since $\rho_p(r)$ is negative, practically any static PPS process[12] will result in a net red shift. For example, substitution into (9) of $\rho_p(r) = -2(Z-1)e^3N_e/rkT$, the first published PPS model,[4] yields a red shift equal in magnitude but opposite in sign to the shift originally derived from the shielding term alone. This model is equivalent to the first-order Debye model, and the shift is given by (7).

Ion quadrupole effects (second-order multipole term in the emitter-ion perturber interaction) yield blue shifts for the He II Paschen lines which are large enough to result in net red shifts that are about 50% smaller than the Debye polarization shifts. With use of the theory of Demura and Sholin[13] it is possible to derive expressions for the quasistatic ion quadrupole shift, δ^q, at $\Delta\omega$ from line center,

$$\delta^q(\Delta\omega) = \int_0^{\beta_{\max}} d\beta H(\beta) \frac{\sum_k W_k(\beta,\Delta\omega)\Delta\omega_k{}^q(\beta)}{\sum_k W_k(\beta,\Delta\omega)}, \tag{10}$$

where

$$W_k(\beta,\Delta\omega) = \frac{\gamma_k}{\pi} \frac{[I_k{}^0 + \Delta I_k(\beta)]}{[\Delta\omega_k{}^d(\beta) + \Delta\omega_k{}^q(\beta) - \Delta\omega]^2 + \gamma_k{}^2}. \tag{11}$$

The dipole shift of the kth Stark component is $\Delta\omega_k{}^d$, and the quadrupole shift is

$$\Delta\omega_k{}^q(\beta) = \frac{2\pi}{3} \frac{e^2a_0{}^2}{\hbar Z^2} N_e\beta^{3/2}[n^4 - n^2 - 6n^2(n_1-n_2)^2 - n'^4 + n'^2 + 6n'^2(n_1'-n_2')^2]T(\beta) \tag{12}$$

where n, n_1, and n_2 are the parabolic quantum numbers. The function

$$T(\beta) = \frac{1}{2\beta^{3/2}}\left[\frac{3\int_0^\beta H(\beta')d\beta'}{\beta H(\beta)} - 1\right] \tag{13}$$

expresses the many-body correction to the "nearest-neighbor" field gradient; it approaches zero as $\beta \to 0$, and one as $\beta \to \infty$. The intensity corrections are

$$\Delta I_k{}^q/I_k{}^0 = (a_0/ZR_0)\beta^{1/2}\epsilon_k T(\beta), \tag{14}$$

where the ϵ_k are given in Ref. 13, and $\frac{4}{3}\pi R_0{}^3 = N_e{}^{-1}$. The distribution $H(\beta)$ of the normalized microfield β at a charge point[14] was interpolated to our experimental conditions. We set $\beta_{\max} = 40$, which is roughly determined by the multipole validity criterion that $n^2a_0/ZR_0 \ll \beta^{-1/2}$. We estimated the impact widths, γ_k, by finding the value which, when convolved with the quasistatic ion distribution, produced a Paschen α line width equal to the measured value. The impact widths for Paschen β and γ lines were scaled by approximately $\gamma \sim n^4$. The ion quadrupole shifts were insensitive to the values of $\beta_{\max}$ and γ_k, the only two parameters which had any latitude in the values assigned them. We also included contributions arising from the quadratic Stark effect, the second-order perturbative term of the quadrupole interaction, and the octupolar term. However, as pointed out by Sholin,[15] these contributions are usually small compared with the first-order quadrupole shift as long as the validity criterion is satisfied. In our experiment we took the shift of the line to be the distance of the bisector of the line at the half width from the unperturbed line center:

$$\Delta\lambda^q/\lambda = -[\delta^q(\Delta\omega_{-1/2}) + \delta^q(\Delta\omega_{+1/2})]\lambda/4\pi c. \tag{15}$$

Figure 1 shows the net computed shifts to be (15–30)% less than the measured ones. These differences are less than present theoretical uncertainties and do not necessarily preclude a significant role by additional shift mechanisms. Estimates for the contributions from "trivial" sources,[10] and unresolved dielectronic satellites proved to be negligible. However, significant red shifts have been shown to arise from strong electron collisions for Lyman α line of He II (Ref. 16) and H_α of H I,[17] as well as from "close-encounter" polarization (CEP) effects for neutrals.[18] We have extended the CEP theory to the case of a charged emitter; the perturbation potential can be expressed as the sum of the Debye term [Eq. (3)], which vanishes for neutrals, plus CEP terms analogous to those in Ref. 18. The CEP terms for ions correct for the more drastic approximations made in the Debye model, i.e., exponentials in the interaction energy over kT are not linearized and the bound electron is treated as such, rather

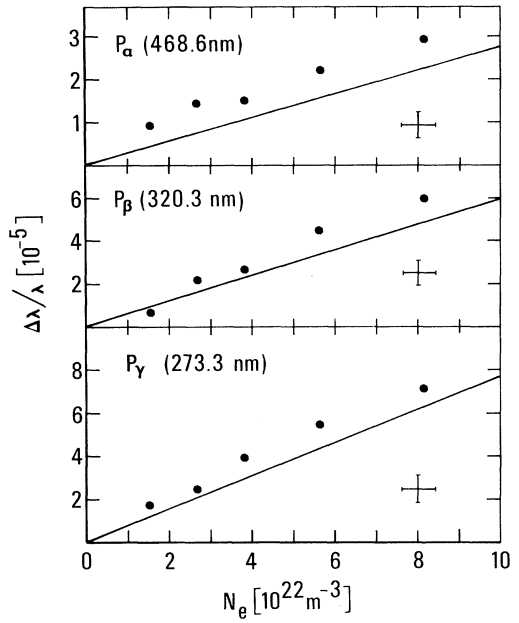

FIG. 1. Red shifts per transition wavelength vs electron density, N_e, for the ($n = 4, 5, 6 \rightarrow n' = 3$) lines of He II. Computed shifts (solid line) include ion quadrupole shifts [Eq. (15)], and plasma polarization shifts, estimated from the Debye model [Eq. (7)]. Calculated values are for an equal density of singly and doubly charged ions.

than as a point charge at the ion nucleus. Computations of the electron and CEP contributions for He II are planned. However, the need for a full dynamical many-body quantum solution to the problem still exists. Further experimental work on the shifts is also required, especially on the T and Z dependence.

We are pleased to acknowledge the continued support and advice of W. L. Wiese, J. R. Roberts, L. Roszman, and J. Cooper.

[1]R. L. Greene, Phys. Rev. A 19, 2002 (1979).
[2]K. Y. Shen and J. Cooper, Astrophys. J. 155, 37 (1969).
[3]J. T. O'Brien and C. F. Hooper, J. Quant. Spectrosc. Radiat. Transfer 14, 479 (1974).
[4]H. F. Berg, A. W. Ali, R. Lincke, and H. R. Griem, Phys. Rev. 125, 199 (1962); H. F. Berg, Z. Phys. 191, 503 (1966).
[5]E. A. M. Baker and D. D. Burgess, J. Phys. B 12, 2097 (1979).
[6]S. Volonte, J. Phys. D 11, 1615 (1978).
[7]H. R. Griem, *Spectral Line Broadening by Plasmas* (Academic, New York, 1974).
[8]R. W. Lee, J. Phys. B 12, 1129 (1979).
[9]A. R. Jacobson and D. L. Call, Rev. Sci. Instrum. 49, 318 (1978).
[10]H. R. Griem, *Plasma Spectroscopy* (McGraw-Hill, New York, 1964).
[11]H. A. Bethe and E. E. Salpeter, *Quantum Mechanics of One- and Two-Electron Atoms* (Academic, New York, 1957).
[12]We must exclude the class of solutions for which $-3 < k_{\min} \leq -2$ near the origin, for which (8) is defined but (9) is not; in this case the value of $\rho_p(r)$ for all r must be known to establish the sign of the shift. We also note that when the lower level is shifted more than the upper (e.g., in some $\Delta n = 0$ transitions), a blue shift results.
[13]A. V. Demura and G. V. Sholin, J. Quant. Spectrosc. Radiat. Transfer 15, 881 (1975).
[14]J. T. O'Brien and C. F. Hooper, Phys. Rev. A 5, 867 (1972).
[15]G. V. Sholin, Opt. Spectrosc. 26, 275 (1969).
[16]K. Yamamoto and H. Narumi, J. Phys. Soc. Jpn. 44, 349 (1978).
[17]M. E. Bacon, Phys. Rev. A 3, 825 (1971).
[18]O. Theimer and P. Kepple, Phys. Rev. A 1, 957 (1970).